AGU PUBLICATIONS

JGR

Journal of Geophysical Research: Biogeosciences

RESEARCH ARTICLE
10.1002/2015JG002972

Key Points:
- Interannual variation of winter mixing controls profundal CH_4 production
- Substantial CH_4 oxidation was observed in aerobic and anaerobic water columns
- CH_4 produced in sediment was mostly oxidized before reaching the water surface

Correspondence to:
M. Itoh,
masayukiitoh@yahoo.co.jp

Citation:
Itoh, M., Y. Kobayashi, T.-Y. Chen, T. Tokida, M. Fukui, H. Kojima, T. Miki, I. Tayasu, F.-K. Shiah, and N. Okuda (2015), Effect of interannual variation in winter vertical mixing on CH_4 dynamics in a subtropical reservoir, *J. Geophys. Res. Biogeosci.*, *120*, doi:10.1002/2015JG002972.

Received 25 FEB 2015
Accepted 26 MAY 2015
Accepted article online 1 JUN 2015

Effect of interannual variation in winter vertical mixing on CH_4 dynamics in a subtropical reservoir

Masayuki Itoh[1], Yuki Kobayashi[2,3], Tzong-Yueh Chen[2], Takeshi Tokida[4], Manabu Fukui[5], Hisaya Kojima[5], Takeshi Miki[2,6], Ichiro Tayasu[3], Fuh-Kwo Shiah[2], and Noboru Okuda[3]

[1]Center for Southeast Asian Studies, Kyoto University, Kyoto, Japan, [2]Research Center for Environmental Changes, Academia Sinica, Taipei, Taiwan, [3]Research Institute for Humanity and Nature, Kyoto, Japan, [4]National Institute for Agro-Environmental Sciences, Tsukuba, Japan, [5]Institute of Low Temperature Science, Hokkaido University, Sapporo, Japan, [6]Institute of Oceanography, National Taiwan University, Taipei, Taiwan

Abstract Although freshwaters are considered to be substantial natural sources of atmospheric methane (CH_4), in situ processes of CH_4 production and consumption in freshwater ecosystems are poorly understood, especially in subtropical areas, leading to uncertainties in the estimation of global CH_4 emissions. To improve our understanding of physical and biogeochemical factors affecting CH_4 dynamics in subtropical lakes, we examined vertical and seasonal profiles of dissolved CH_4 and its carbon isotope ratio ($\delta^{13}C$) and conducted incubation experiments to assess CH_4 production and oxidation in the deep subtropical Fei-Tsui Reservoir (FTR; Taiwan). The mixing pattern of the FTR is essentially monomixis, but the intensity of winter vertical mixing changes with climatic conditions. In years with incomplete vertical mixing (does not reach the bottom) and subsequent strong thermal stratification resulting in profundal hypoxia, we observed increases in sedimentary CH_4 production and thus profundal CH_4 storage with the development of reducing conditions. In contrast, in years with strong winter vertical mixing to the bottom of the reservoir, CH_4 production was suppressed under NO_3^--rich conditions, during which denitrifiers have the competitive advantage over methanogens. Diffusive emission from profundal CH_4 storage appeared to be negligible due to the efficiency of CH_4 oxidation during ascent through methane-oxidizing bacteria (MOB) activity. Most of the profundal CH_4 was rapidly oxidized by MOB in both oxic and anoxic layers, as characterized by its carbon isotope signature. In contrast, aerobic CH_4 production in the subsurface layer, which may be enhanced under high temperatures in summer, may account for a large portion of atmospheric CH_4 emissions from this reservoir. Our CH_4 profiling results provide valuable information for future studies predicting CH_4 emissions from subtropical lakes with the progress of global warming.

1. Introduction

Methane (CH_4) is a key greenhouse gas (GHG) that has an infrared radiative heating effect 28 to 34 times greater than carbon dioxide (CO_2) on a mass basis on a 100 year time horizon [*Intergovernmental Panel on Climate Change*, 2013]. Natural sources of CH_4 account for about 35–50% of mean global CH_4 emissions over recent decades [*Ciais et al*., 2013]. Freshwaters are a primary natural source of atmospheric CH_4. According to the meta-analysis of *Bastviken et al*. [2011], lakes, reservoirs, and rivers emit 103 Tg of $CH_4\,yr^{-1}$, which is 0.65 Pg of C (expressed as CO_2 equivalent) and equal to 25% of the estimated terrestrial GHG sink. In their analysis, the available data are biased toward boreal and temperate regions: the proportion of case studies in tropical and subtropical open freshwaters (at latitudes $<24°$) is less than one tenth (40 of 474 cases). Due to high water temperatures and meromixis (i.e., thermal stratification throughout the year), tropical lakes have high potential for CH_4 production in anoxic deep waters and sediment [e.g., *Pasche et al*., 2011]. In contrast, subtropical lakes experience vertical mixing in winter when recovering from hypoxia in deep water, which can decrease the potential for CH_4 production by methanogens in the sediment and can facilitate CH_4 oxidation by methane oxidizing bacteria (MOB) within the water column. However, little information exists regarding CH_4 dynamics related to environmental factors in subtropical lakes. Therefore, the processes of CH_4 production, oxidation, and emission in subtropical freshwaters should be assessed to contribute to better estimations of global CH_4 emissions.

Recently, CH_4 emissions from reservoirs, especially hydroelectric reservoirs, have been reported in boreal [*Teodoru et al*., 2012], temperate [*Chen et al*., 2011; *Xiao et al*., 2013], subtropical [*Chanudet et al*., 2011], and

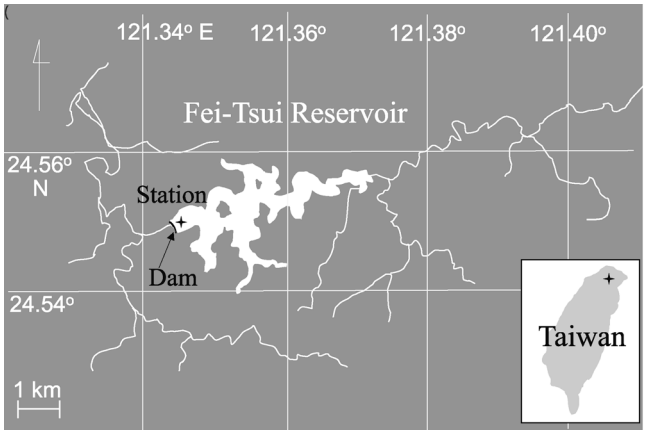

Figure 1. Location of the sampling site at the Fei-Tsui Reservoir (FTR) in northern Taiwan.

tropical [*Abril et al*., 2005; *Guérin and Abril*, 2007] regions. A meta-analysis of published data on hydroelectric reservoirs, which account for about 20% of all reservoirs worldwide in terms of area, estimated that they emit 48 Tg C as CO_2 or 3 Tg C as CH_4 [*Barros et al*., 2011]. However, most of these reports only focused on CH_4 emissions from water surfaces, and only a few studies have examined CH_4 production and oxidation in the water column and sediment [e.g., *Guérin and Abril*, 2007]. Because CH_4 emission from the water surface depends not only on the biogeochemical processes of CH_4 production and oxidation but also on the physical processes of CH_4 transportation, the identification of both physical and biogeochemical factors affecting CH_4 dynamics will provide a better understanding of the mechanisms that control CH_4 emission from lakes and reservoirs.

The deep subtropical Fei-Tsui Reservoir (hereafter, FTR) is among the largest reservoirs in northern Taiwan (Figure 1). The FTR is an interesting system because it is located in a subtropical region and its mixing pattern is essentially monomixis (characteristic of subtropical lakes); however, the intensity of winter mixing frequently changes with climatic conditions. In subtropical monomictic lakes, ongoing global warming could potentially increase the intensity and duration of thermal stratification in summer and weaken vertical mixing in winter [*Sahoo and Schladow*, 2008; *Yoshimizu et al*., 2010], both of which can facilitate CH_4 production at the lake bottom but prevent the upward advection of profundal dissolved CH_4. The overall effect of a warming climate on CH_4 emission from subtropical lakes is poorly understood. Therefore, our comparison of CH_4 dynamics in this reservoir between strong and weak winter mixing years will provide insight into how ongoing global warming will affect CH_4 emissions from lake ecosystems at a wide latitudinal scale.

In the present study, we examined vertical and seasonal profiles of dissolved CH_4 and its carbon isotope ratio ($\delta^{13}C$) and conducted incubation experiments to examine the dynamic processes of CH_4 in the water column and surface sediment of FTR. Values of $\delta^{13}C$-CH_4 have been used as evidence of CH_4 oxidation by MOB [e.g., *Bastviken et al*., 2002; *Blees et al*., 2014; *Morana et al*., 2015]. Using this isotope technique, particularly $\delta^{13}C$-CH_4 values for low concentrations of CH_4 in the water column, our objective was to understand the mechanisms controlling CH_4 production/oxidation in a deep subtropical reservoir.

2. Materials and Methods

2.1. Study Site and Sampling Design

The FTR (121°34′E, 24°54′N) is located downstream of Peishih Creek and resides in a watershed area of 303 km^2 in northern Taiwan (Figure 1). Annual mean air temperature at this reservoir during the monitoring years (2004–2013) was 21.5°C. The lowest monthly mean air temperature in winter (December to February) varied from 11.8 to 15.7°C, whereas the highest air temperature in summer (July or August) was less variable among monitoring years (range: 27.9 to 28.7°C). Annual precipitation at the FTR from 2004 to 2013 ranged from 3518 to 4774 mm (mean: 4052 mm). Although the region experiences typhoons every summer, the amount of summer to autumn precipitation varies from year to year (Figure 2a). Mixing was observed during the coolest period of the year; however, its intensity varied annually. The FTR is the major drinking water source for 5 million people living in metropolitan Taipei and its suburbs. The reservoir was constructed in 1987 and is protected from human activities. Therefore, the FTR is considered an artificial semiclosed lacustrine system. The FTR has a surface basin area of 10.24 km^2 and a designed total water storage

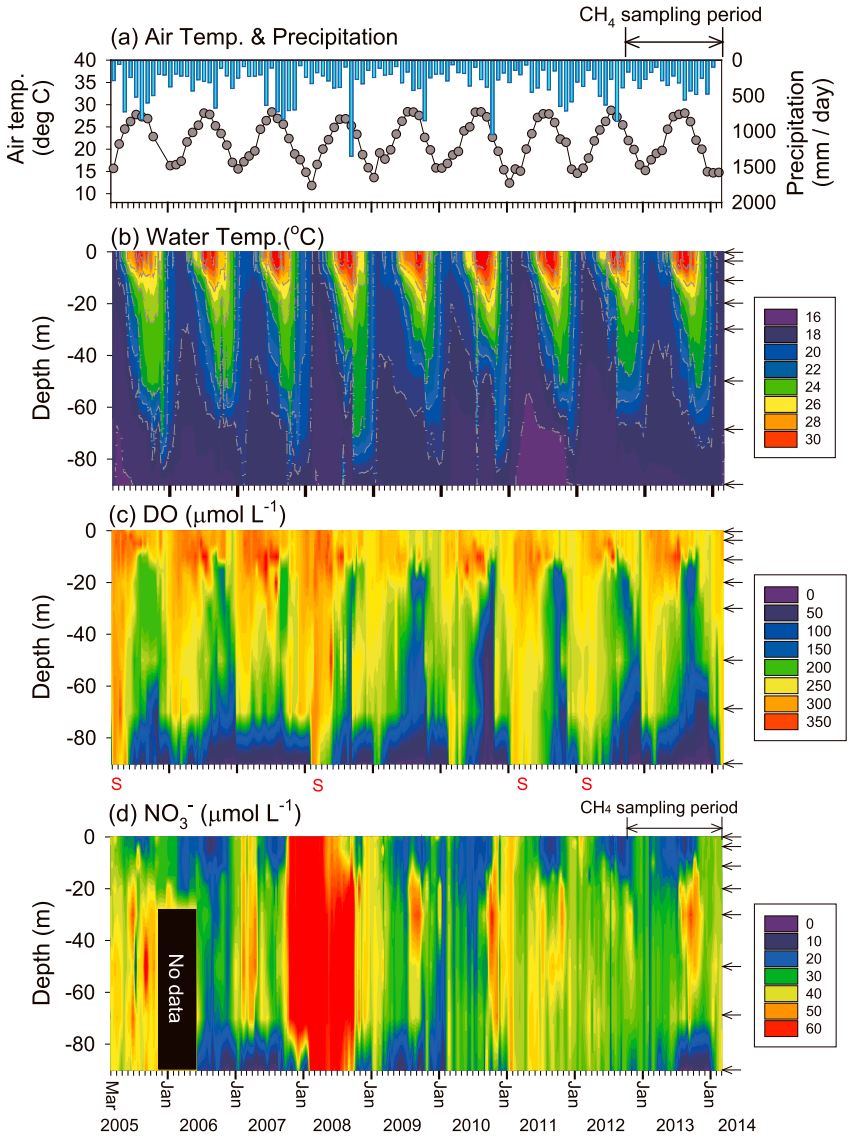

Figure 2. The long-term monitoring of seasonal variation in (a) monthly averaged air temperature and precipitation at the Fei-Tsui Reservoir (FTR) and biweekly changes in the vertical distribution of (b) water temperature, (c) dissolved oxygen (DO), and (d) NO_3^- concentration in the FTR. Horizontal arrows indicate the sampling depths for the present study. S under Figure 2c indicates strong winter mixing.

capacity of $406 \times 10^6\,m^3$ at its normal maximum water surface elevation of 170 m above sea level (asl). The average slope of the reservoir bed is 0.3%, the mean depth is 39.4 m, and the maximum depth is 113.5 m at the dam. The water level fluctuates from 144 to 168 m asl. Three water intakes are located near the dam at depths of 108, 128, and 148 m asl. The average water residence time is 115 days [*Chen et al.*, 2006]. According to long-term records of Carlson's trophic state index, the FTR is classified as a mesotrophic lake [*Chou et al.*, 2007]. The depth of the euphotic zone ranges from 10 to 20 m.

In 2005, we began long-term monitoring of the physicochemical environment on a weekly or biweekly basis at 10 depths (0, 2, 5, 10, 15, 20, 30, 50, 70, and 90 m from the water surface) at a sampling station (Figure 2) located 250 m from the FTR dam (Figure 1). Vertical profiles of water temperature were recorded using a conductivity, temperature, and depth logger (Idronaut, Brugheiro, Italy) equipped with an automated lift. Long-term precipitation, air temperature, and wind speed data were available from the Taipei Feitsui Reservoir Administration (http://english.fra.taipei.gov.tw).

2.2. CH_4 Concentration and Its $\delta^{13}C$

We focused on seasonal variation in CH_4 from 2012 to 2014, during which the intensity of winter vertical mixing alternated from strong to weak: strong mixing in the winter seasons of 2011–2012 and 2013–2014 and weak mixing in the winter 2012–2013 (Figure 2). For measurements of dissolved CH_4 concentration and its $\delta^{13}C$, we conducted water sampling on a weekly or biweekly basis from October 2012 to February 2014. Water samples were collected from six depths (0, 10, 30, 50, 70, and 90 m from the water surface) using a 5 L Go-Flo bottle (General Oceanics, Miami, FL, USA). We also collected additional samples from a depth of 80 m from February to June 2013 and from near the bottom (hereafter, "near bottom") from February 2013 to February 2014. The depths of the near-bottom samples ranged from 95 to 100 m, depending on the water level of the reservoir.

Water samples were divided into two subsamples: one was placed into a 20 or 30 mL glass vial for measurement of dissolved CH_4, while the other was placed into a plastic bottle for measurements of other chemicals. Vials and plastic bottles were stored in a cooler (~4°C) immediately after sampling. The glass vials were completely filled, plugged with butyl rubber stoppers, and then sealed with aluminum caps with no exposure to the atmosphere. Within 3 h after sampling, 0.1 mL of a saturated mercuric (II) chloride ($HgCl_2$) solution was added to the vials and bottles to inhibit microbial activity in the water samples. Dissolved CH_4 concentrations were measured using multiple equilibrations with a headspace of ultrahigh-purity (UHP) helium [*McAuliffe*, 1971]. Within a vial bottle, the headspace was prepared by replacing sampled water with He (>99.999% purity). The vials were vigorously shaken for 2 min to drive gases from the water into the headspace. The headspace gas was removed using a gastight syringe, and the CH_4 concentration was then determined using a gas chromatograph (GC; GC2014, Shimadzu, Japan) equipped with a flame ionization detector (FID) and a thermal conductivity detector (TCD) [*Itoh et al*., 2011].

For the carbon isotope analysis of dissolved CH_4 ($\delta^{13}C$-CH_4), the same water that was sampled for concentrations of CH_4 and other chemicals was placed in 125 mL glass vials or 500 mL polyethylene terephthalate bottles. The protocol for gas sample treatment was the same as that for measurements of CH_4 concentration. The headspace was transferred to a preevacuated small glass bottle and analyzed using a gas chromatograph/combustion/isotope ratio mass spectrometer (GC/C/IRMS) (Thermo Finnigan MAT252: Thermo Fisher Scientific, Waltham, MA, USA) equipped with an HP G1530A (Agilent, Santa Clara, CA, USA) GC system [*Sugimoto*, 1996] at the Center for Ecological Research (CER) at Kyoto University [*Itoh et al*., 2008]. For this GC/C/IRMS at the CER, the precision of repeated analysis was ±0.19‰ when 44 nmol of CH_4 was injected. For low CH_4 concentration samples, $\delta^{13}C$-CH_4 was determined using GC/C/IRMS (Delta V advantage, Thermo Fisher Scientific) with a cryofocus trap at the National Institute for Agro-Environmental Sciences (NIAES), Japan [*Tokida et al*., 2014]. For this GC/C/IRMS at the NIAES, the precision of repeated analysis was ±0.11‰ when 1.6 nmol of CH_4 was injected.

2.3. DO and NO_3^- Concentrations

For measurements of dissolved oxygen (DO), water samples were collected into 100 mL biological oxygen demand bottles and then fixed immediately after sampling. DO was determined following the Winkler method. For measurements of NO_3^-, water samples were filtered using GF/F filters (ϕ0.7 μm, Whatman, Maidstone, UK) and measured following the protocol of *Parsons et al*. [1984] using flow injection analysis.

2.4. Potential CH_4 and CO_2 Production in the Sediment

To determine the seasonal variation in methanogenic and microbial activity in the sediment, sediment samples from the lake bottom were collected at the sampling station in winter (11 December 2012) and summer (30 July 2013). Duplicate sediment samples (referred to as Sediment 1 and Sediment 2) were collected from the surface of the lake bottom (approximately 0–5 cm depth) using an Ekman-Berge sampler. Samples were immediately sealed in airtight plastic bags and stored in a cooler (~4°C) prior to incubations to estimate potential CH_4 and CO_2 production under anaerobic conditions. After the homogenization of sediment samples, which were composed of fine silts, total C and total N contents

and $\delta^{13}C$ values were measured using a mass spectrometer (DELTA V and DELTA V Advantage, Thermo Fisher Scientific) coupled with an elemental analyzer (Flash EA, Thermo Fisher Scientific).

We conducted anaerobic incubations of the surface sediment to estimate potential CH_4 and CO_2 production under anaerobic conditions, referring to the procedure of *Itoh et al.* [2011]. Nine replicates of wet sediment samples (approximately 10 g) for both Sediment 1 and Sediment 2 were waterlogged in 10 mL of distilled water in 50 mL glass vials, which were sealed with butyl rubber stoppers. The slurry was purged with pure N_2 gas using a long needle to reach the bottom of the vial, and the headspace gas and the gas trapped in the sediment were completely replaced. Vials were incubated under dark and static conditions, simulating the water temperature of the deepest measurement depth (90 m) at the sampling time (17°C for both experiments). For each measurement, the vials were shaken gently, and gaseous CH_4 and CO_2 present in the vial headspace were then injected into the GC-FID-TCD using a gastight syringe. Measurements were made immediately after sealing the vial within 5 days of incubation. Each measurement was conducted at 0 (immediately after purging), 1, 2, and 5 days after purging. Potential CH_4 and CO_2 production under anaerobic conditions were calculated from the changes in concentrations and were expressed on a dry soil basis (oven dried at 105°C for 48 h).

2.5. CH_4 Oxidation in the Water Column

The methane oxidation rate in the water column was defined as the specific decrease of the dissolved CH_4 concentration (nmol h^{-1} L^{-1}) using a linear function of CH_4 concentration against incubation time during the early stage of the incubation period, assuming that this period was similar to natural conditions. We collected water samples from depths of 0, 10, 30, 50, 70, and 90 m in winter (11 December 2012) and summer (30 July 2013). At each depth, duplicate 20 mL glass vials were completely filled for each time series. After sealing the vials with butyl rubber stoppers and aluminum caps, 0.1 mL of saturated $HgCl_2$ was immediately added to two vials (controls), and all vials were incubated in the dark. At each time interval, two vials were sacrificed by the addition of $HgCl_2$ to inhibit microbial activity at seven time intervals within 24 h of incubation (e.g., 1, 2, 4, 8, 16, and 24 h). Dissolved CH_4 concentrations were measured using the same method as described in section 2.2. For each sample, the temperature during incubation was adjusted to be within 1°C of the temperature at the sampling depth and time.

To determine an enrichment factor for CH_4 oxidation in the water column, we conducted a 12 day water incubation experiment, with the addition of CH_4 gas. For the above incubation experiments, we used water samples from 70 m depth, at which CH_4 oxidation rates were among the highest in the water column in both summer and winter. Water samples were collected in 20 mL glass vials in triplicate on 25 February 2014, when the water column was well mixed down to the deepest layer. After sealing the vials with butyl rubber stoppers and aluminum caps, 1.5 mL of headspace of ultrahigh-purity (UHP) helium was created, and 3 μL of 99% CH_4 was added to the headspace. This addition of CH_4 gas was equivalent to an increase of approximately 9 μmol L^{-1} in the dissolved CH_4 concentration of the water samples under equilibrium conditions, which was within the maximum CH_4 concentration previously observed at depths of 70 and 90 m. Incubations were conducted under dark conditions for 12 days. After 1, 2, 4, 8, and 12 days of incubation, $HgCl_2$ solution was added to each of the triplicate samples to inhibit microbial activity. After measurements of dissolved CH_4 concentrations and $\delta^{13}C$ values, the specific CH_4 oxidation rate (nmol h^{-1} L^{-1}) was determined in the same way as described above but using the concentrations of the entire 12 days of incubation.

Apparent kinetic isotope enrichment factors for CH_4 oxidation were calculated using the Rayleigh model for a closed system [*Mariotti et al.*, 1981] as follows:

$$\varepsilon_{\mathrm{closed}} = \frac{10^3 \ln \frac{10^{-3}\delta_S + 1}{10^{-3}\delta_{S,0} + 1}}{1 - f} \quad (1)$$

where ε is the enrichment factor (in per mil) between the product and substrate; δ_S and $\delta_{S,0}$ are the $\delta^{13}C$ values of CH_4 at each incubation time and at the initial time (1 day after the onset of incubation), respectively; and f is the fraction of CH_4 remaining.

2.6. Estimation of Diffusive CH_4 Flux

To determine the seasonal pattern in diffusive CH_4 flux, CH_4 exchange at the water surface (i.e., diffusive CH_4 flux) was estimated at each sampling on the basis of atmospheric equilibrium solubility and fractional saturation. The theoretical atmospheric equilibrium solubility of dissolved CH_4 was calculated according to the equation of *Wiesenburg and Guinasso* [1979].

The diffusive CH_4 flux was calculated by the boundary layer model using the equation of *Wanninkhof* [1992]:

$$F = k\ (C_w - C_a), \tag{2}$$

where F is the diffusive CH_4 flux across the air-water interface (mol m^{-2} d^{-1}), k is the gas transfer velocity (m d^{-1}), C_w is the measured gas concentration in the bulk water near the interface (0 m depth) (mol m^{-3}), and C_a is the gas concentration in the air phase near the interface. *Schubert et al*. [2012] suggested that the calculated diffusive flux varies depending on the value of k derived from a different formula. Because the wind speed-gas transfer velocity is considered to be site specific [e.g., *Borges et al*., 2004; *Guérin et al*., 2007; *Vachon and del Giorgio*, 2014], we used two different formulas for the calculation of k_{600}, which is the gas transfer velocity normalized to a Schmidt number (Sc) of 600, to determine the possible range of the diffusive CH_4 flux:

$$k_{600} = 0.72\ U_{10},\ \text{cm h}^{-1},\ \text{for U}_{10} < 3.7\ \text{m s}^{-1}\ [\textit{Crusius and Wanninkhof},\ 2003] \tag{3}$$

and

$$k_{600} = 2.07\ +\ 0.215\ U_{10},\ \text{cm h}^{-1},\ \text{for U}_{10} < 3\ \text{m s}^{-1}\quad [\textit{Cole and Caraco},\ 1998] \tag{4}$$

where U_{10} is the wind speed at 10 m height (which was always less than 3 m s^{-1} in our site).

The k_{600} was then transformed into the transfer velocity k for CH_4 using the following equation [*Jähne et al*., 1987]:

$$k600 = k_{g,T}\left(600/Sc_{g,T}\right)^{-n}, \tag{5}$$

where $k_{g,T}$ and $Sc_{g,T}$ are the k and the Schmidt number of the given gas (CH_4) at the water surface temperature [*Wanninkhof*, 1992], respectively, and n is −⅔ for wind speeds less than 3.7 m s^{-1} and −½ for higher wind speeds [*Liss and Merlivat*, 1986; *Jähne et al*., 1987], although the average wind speed used in this study was always less than 3.7 m s^{-1}.

We did not measure the atmospheric CH_4 concentration for C_a at every sampling; therefore, we used the atmospheric CH_4 concentration (1.76 ppmv) measured just above the water surface of the FTR on 30 July 2013, under the assumption that the atmospheric CH_4 concentration just above the water surface was stable. The dissolved CH_4 concentration at a depth of 0 m on each sampling date was C_w. A 1 day average of wind speed on the sampling date was used in the flux calculation. To determine the general trend of the diffusive CH_4 flux, an 11 day average (day 6 was the sampling date) of wind speed was also used in the diffusive CH_4 flux calculation and compared with the results using a 1 day average, considering that the diffusive CH_4 flux depended heavily on wind speed.

Linear regression was conducted with the Sigma Plot 11.0 software package (SPSS, Chicago, IL, USA). Specific differences among the groups were analyzed using Tukey's multiple comparison test, using the statistical software R, version 2.15.1 [*R Development Core Team*, 2012].

3. Results

3.1. Interannual Variation in Climate and Water Stratification

Mixing was observed at the end of the coolest period of the year, usually from January to March; however, its intensity varied annually. Here we consider that the DO level at the bottom layer is a good indicator of mixing (Figure 2c). Apparent penetrations of high DO levels to the deep zone (90 m depth) were observed in the winters of 2004–2005, 2007–2008, 2010–2011, and 2011–2012 (shown in "S" in Figure 2c). However, the duration and intensity of DO penetration to 90 m depth were variable (Figure 2c). Linear regression analysis indicated that average surface water temperature during winter (December to February) was

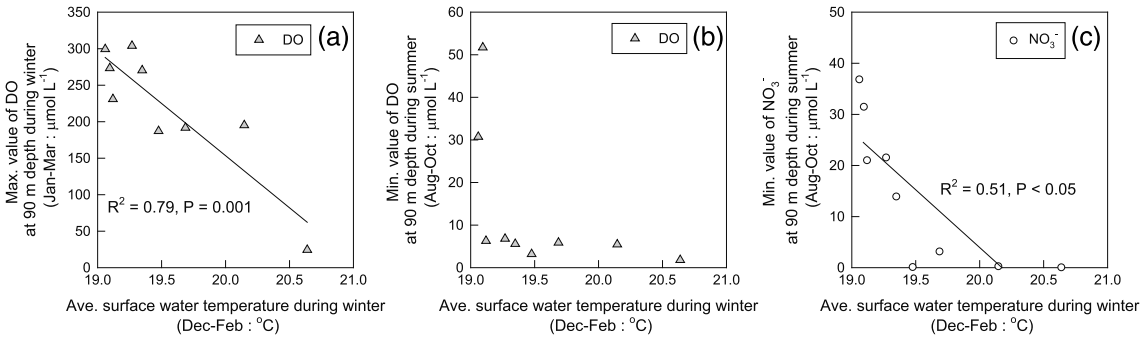

Figure 3. Results of regression analyses between average surface water temperature during winter (December to February) versus (a) the maximum profundal DO concentration in winter (with 1 month lag time) and the minimum profundal (b) DO and (c) NO_3^- concentration during the following stratification period (August to October).

significantly related to maximum DO value at 90 m depth from January to March ($R^2 = 0.79$, $P = 0.001$ for 9 year data; Figure 3a). These results indicate that the penetration of high DO to deeper layers due to stronger mixing was observed during cool winters (Figure 2c). Therefore, surface water temperature during the winter affects the intensity of winter mixing, and thus DO conditions, in the deep zone with a 1 month lag time. Using a 9 year observational data set for the FTR, the total precipitation during the end of the warm wet season/beginning of the cool dry season (hereafter, cooling periods; from October to December) and average surface water temperature during the following winter indicated that the higher amounts of precipitation during the cooling period (mainly due to typhoons) induced the lower surface water temperatures in winter ($R^2 = 0.55$, $P < 0.05$).

These observations indicated that (1) stratification can be maintained even during a winter with a high surface water temperature (i.e., weak mixing), and (2) a low surface water temperature (after high precipitation) induces more intense mixing (Figures 2a and 2c). In turn, the incomplete vertical mixing in winter sustained reducing condition at the bottom layer and decreased profundal DO and NO_3^- concentration during the following summer (Figures 2c, 2d, 3b, and 3c), as oxygen depletion occurred during the following thermal stratification period and facilitated NO_3^- consumption by denitrifiers (Figure 2d).

3.2. CH_4 Concentration and Its $\delta^{13}C$ Values

At the end of the stratification period in 2013, CH_4 concentrations in deep waters reached 343.0 μmol L^{-1} and profundal CH_4 storage developed under extremely low NO_3^- conditions (Table 1 and Figures 2d, 4a, and 5b) after the weak mixing in winter 2012–2013. Such CH_4 accumulation was not observed after strong vertical mixing in the winter 2011–2012 (Figures 2, 4a, and 5a). Although no CH_4 concentration data were available for the near bottom during the cooling period of 2012 (October to December), CH_4 concentrations at 90 m depth during the cooling period significantly differed ($P < 0.0001$) between 2012 (0.11 ± 0.23 μmol L^{-1}, mean ± SD) and 2013 (84.0 ± 25.4 μmol L^{-1}). Incomplete mixing at the end of winter

Table 1. Mean ± SD, Minimum, and Maximum CH_4 Concentrations and $\delta^{13}C$-CH_4 Values (Data From October 2012 to February 2014)

	CH_4 (μmol L^{-1})				$\delta^{13}C$-CH_4 (‰)			
Depth (m)	mean ± SD	min	max	*n*	mean ± SD	min	max	*n*
0	0.036 ± 0.026	0.007	0.093	29	−45.1 ± 5.6	−54.2	−32.3	28
10	0.053 ± 0.042	0.005	0.157	29	−43.0 ± 5.6	−53.0	−29.6	28
30	0.022 ± 0.017	0.007	0.065	29	−38.3 ± 7.0	−53.6	−24.3	29
50	0.013 ± 0.014	0.002	0.062	29	−45.5 ± 6.8	−56.8	−24.7	28
70	0.026 ± 0.041	0.001	0.175	29	−45.4 ± 10.4	−59.7	−7.8	25
80[a]	0.018 ± 0.024	0.003	0.071	7	−43.0 ± 3.0	−46.9	−39.1	7
90	44.3 ± 69.4	0.004	261.7	29	−46.3 ± 18.9	−69.0	−4.4	29
Bottom	135.6 ± 120.1	0.038	343.0	20	−62.6 ± 8.1	−68.0	−33.0	20

[a]Data from February to June 2013.

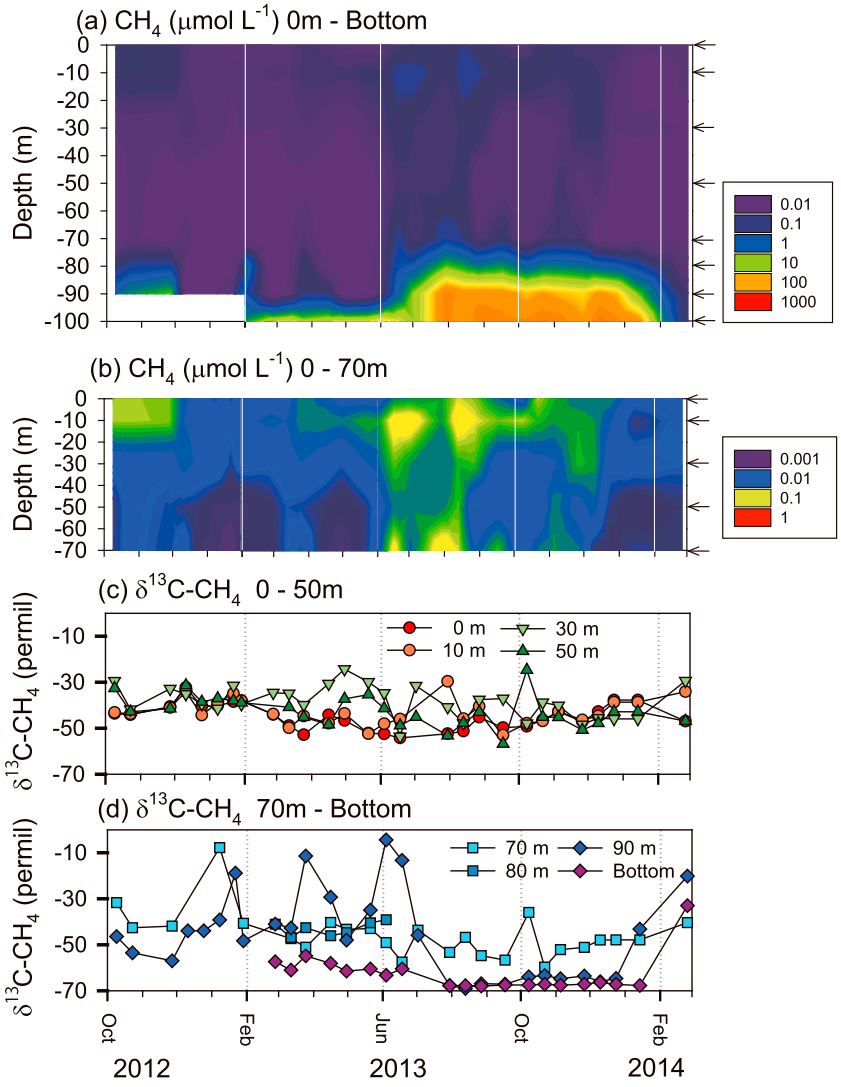

Figure 4. Seasonal variation in (a) dissolved CH_4 concentration from the surface to the bottom; (b) dissolved CH_4 concentration from the surface to 70 m with a smaller CH_4 concentration range; (c) δ^{13}C-CH_4 values at depths of 0, 10, 30, and 50 m; and (d) δ^{13}C-CH_4 values at depths of 70, 80, 90 m, and the near bottom. The horizontal arrows indicate the sampling depths. Note that the near-bottom sampling began in February 2013.

2012–2013 (Figure 5c) helped to sustain low-DO conditions at the deep layer until the following summer (Figure 2c). In contrast, the large CH_4 storage in winter 2013–2014 decreased in the deep layer when the lake waters were vertically well mixed in February 2014 (Figures 4a and 5d).

During the strong stratification period in 2013, dissolved CH_4 concentrations were much lower from 70 m depth to the surface compared to the deeper zone (Figure 5b). During the midsummer season, a small peak of dissolved CH_4 occurred at a depth of 10 m (Figure 4b). This subsurface CH_4 concentration (10 m depth) from June to August 2013 was significantly higher than concentrations at 0 ($P < 0.05$), 30 ($P < 0.05$), and 50 m ($P < 0.005$) depths and much higher than the theoretical atmospheric equilibrium solubility of dissolved CH_4.

The δ^{13}C-CH_4 values at depths of 0–50 m ranged from −56.8‰ to −24.3‰ (Table 1 and Figure 4c), whereas considerably more negative values occurred at the near bottom (−62.6‰ ± 8.1‰; Table 1 and Figure 4d), except after completely mixing in winter 2012–2013 (Figure 2c) and February 2014, when complete mixing occurred (Figure 5d). The near-bottom δ^{13}C-CH_4 values remained at minimum values (mean −67.4‰ ± 0.5‰) during the strongly reduced period with thermal stratification (from August 2013 to January 2014;

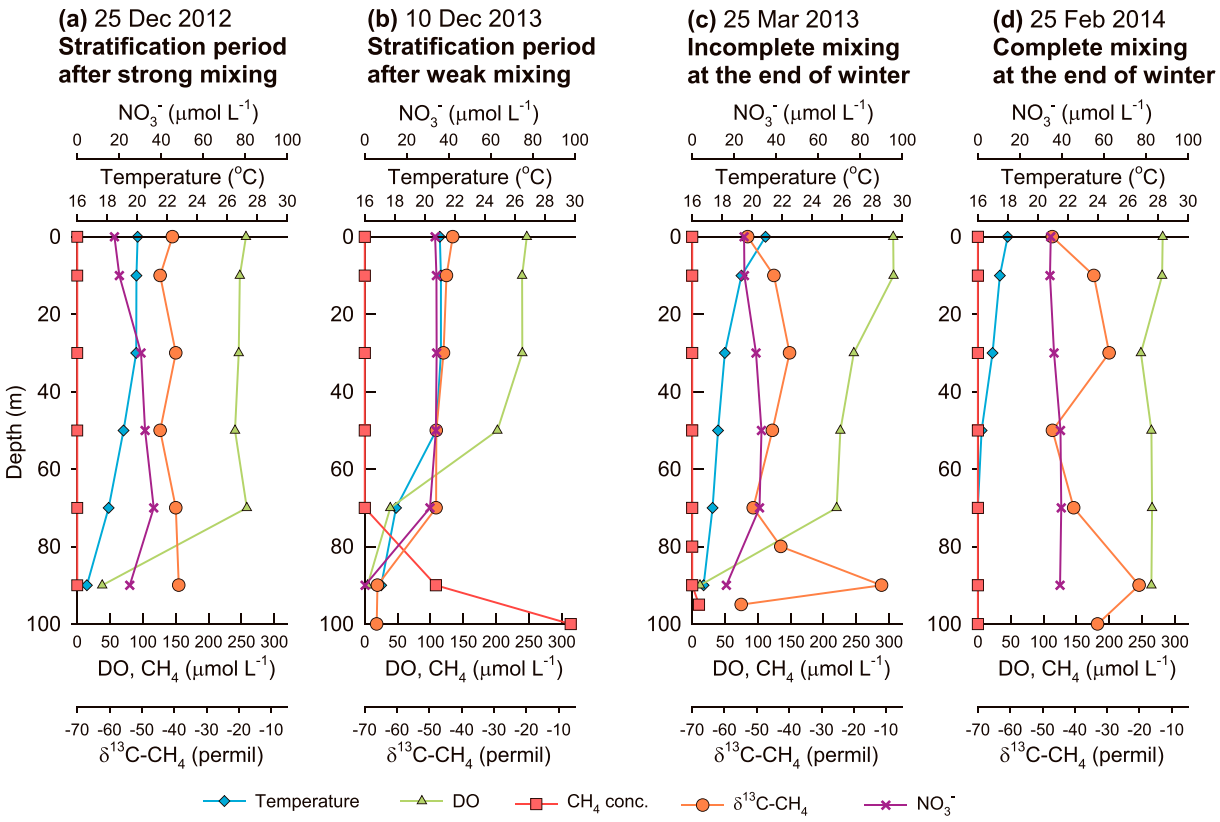

Figure 5. Vertical profiles of water temperature, DO, CH_4 concentration, $\delta^{13}C$-CH_4 values, and NO_3^- concentration on representative sampling dates (a) during the stratification period after complete mixing in winter 2011–2012, (b) during the stratification period after incomplete mixing in winter 2012–2013, (c) during an incomplete mixing at the end of winter 2012–2013, and (d) during a complete mixing at the end of winter 2013–2014. Note that near-bottom sampling began in February 2013.

Figures 4d and 5b). In contrast, at depths of 90 and 70 m, the $\delta^{13}C$-CH_4 values fluctuated substantially, ranging from −69.0‰ to −4.4‰ (90 m) and from −59.7‰ to −7.8‰ (70 m) (Table 1 and Figures 4d, 5b, and 5c). At these two depths, occasional increases in the $\delta^{13}C$-CH_4 values were observed during the early phase of thermal stratification following the strong winter mixing in winter 2011–2012, but not during the late phase of thermal stratification, when strong reducing conditions were maintained in deep waters (Figure 4d).

3.3. Potential CH_4 and CO_2 Production in the Sediments

No marked differences among sampling periods were observed for C and N contents, C/N ratio, or $\delta^{13}C$ values of surface sediment (Table 2). For the lake surface sediment, the potential CH_4 production under anaerobic conditions were significantly lower in winter 2011–2012 than in summer 2013 for all measurement days ($P < 0.001$; Table 3). The potential CO_2 production displayed the same pattern as the potential CH_4 production rates. The potential CO_2 production was significantly lower in the surface sediment in winter 2011–2012 than in summer 2013 for all measurement days ($P < 0.001$; Table 3). Both CH_4 and CO_2 productions were higher on the first day of incubation and decreased throughout incubation.

Table 2. C and N Contents, C/N Ratios, and $\delta^{13}C$ Values of the Surface Sediment

Sampling Period		C (%)	N (%)	C/N	$\delta^{13}C$ (‰)
11 December 2012	Sediment 1	1.21	0.20	6.1	−27.12
	Sediment 2	1.37	0.23	6.1	−27.18
30 July 2013	Sediment 1	1.33	0.19	6.8	−27.20
	Sediment 2	1.09	0.18	6.2	−26.83

Table 3. Results of Surface Sediment Incubation Experiments[a]

Incubation Duration	Sampling Period		Potential CH_4 Production (±SD) (μg CH_4-C g^{-1} dry soil)	Potential CO_2 Production (±SD) (μg CO_2-C g^{-1} dry soil)
Day 1	11 December 2012	Sediment 1	10.0 ± 1.2^a	16.8 ± 0.4^a
		Sediment 2	7.9 ± 1.5^a	19.7 ± 6.0^a
	30 July 2013	Sediment 1	20.9 ± 1.7^b	34.6 ± 9.0^b
		Sediment 2	20.6 ± 3.4^b	33.2 ± 5.1^b
Day 2	11 December 2012	Sediment 1	11.5 ± 1.2^a	20.5 ± 2.7^a
		Sediment 2	9.7 ± 1.6^a	24.0 ± 6.9^a
	30 July 2013	Sediment 1	23.1 ± 5.7^b	38.3 ± 10.3^b
		Sediment 2	21.9 ± 2.3^b	37.3 ± 3.6^b
Day 5	11 December 2012	Sediment 1	17.0 ± 1.2^a	24.9 ± 5.6^a
		Sediment 2	16.6 ± 1.6^a	28.6 ± 6.2^a
	30 July 2013	Sediment 1	25.0 ± 5.9^b	50.1 ± 13.7^b
		Sediment 2	23.5 ± 2.7^b	47.3 ± 6.8^b

[a]Statistically significant differences between samples from the same measurement day are indicated by different letters ($P < 0.001$).

3.4. CH_4 Oxidation Rates in the Water Column

To determine CH_4 oxidation rates, we only used data from samples for which a significantly linear decrease ($P < 0.05$) in CH_4 concentration was observed during the 24 h incubation experiment. Significant linear decreases were observed for water samples from 10, 30, 70, and 90 m depths in winter 2011 (Table 4). In summer 2013, the incubation experiment did not show a significant linear decrease in CH_4 concentrations for water samples from surface to 30 m depth (Table 4). Also, for water samples at a depth of 90 m, whose CH_4 concentrations were very high, the incubation experiment showed a nonlinear change in CH_4 concentration, suggesting that CH_4 concentration was too high to detect CH_4 oxidation by MOB in the vials. At a depth of 70 m, CH_4 oxidation rates were among the highest in the water column in both winter and summer. At this depth, CH_4 concentrations decreased exponentially from 1.98 to 0.03 μmol L^{-1} over 12 days of the incubation experiment in which CH_4 gas was added, with a very significant regression curve ($R^2 = 0.99$; Figure 6a). The initial and final concentrations were within the possible range of in situ dissolved CH_4 concentrations at depths of 70 and 90 m. During the incubation period, δ^{13}C-CH_4 values increased from −28.5‰ ± 0.8‰ at day 1 to 8.5‰ ± 3.5‰ at day 12. Based on the Rayleigh plot, the apparent kinetic isotope enrichment factor ε_{closed} was calculated as −9.27 (Figure 6b).

3.5. Diffusive CH_4 Flux

The dissolved CH_4 concentration at a depth of 0 m remained above the atmospheric equilibrium level throughout the sampling period (Figure 7a). The 1 and 11 day running mean wind speeds ranged from 0 to 2.8 m/s and 0.3 to 2.1 m/s, respectively (Figure 7b). Estimated values of the daily diffusive CH_4 flux from the surface water ranged from 0 to 51.9 μmol m^{-2} d^{-1} and from 0.86 to 29.9 μmol m^{-2} d^{-1} for the 1 and 11 day running means, respectively, according to the formula of *Crusius and Wanninkhof* [2003] (Figure 7c). When the formula of *Cole and Caraco* [1998] was used, the daily diffusive CH_4 flux was estimated as

Table 4. CH_4 Oxidation Rate Determined by Water Incubation Experiments[a]

	11 December 2012				30 July 2013			
Depth (m)	Initial Concentration (nmol L^{-1})	CH_4 Oxidation Rate (nmol h^{-1} L^{-1})	r	P	Initial Concentration (nmol L^{-1})	CH_4 Oxidation Rate (nmol h^{-1} L^{-1})	r	P
0	21.2	n.s.[b]	−0.22	-	46.8	n.s.[b]	0.45	-
10	20.0	6.5	−0.67	<0.05	42.2	n.s.[b]	0.24	-
30	26.0	8.3	−0.57	<0.05	12.2	n.s.[b]	0.11	-
50	5.8	n.s.[b]	−0.39	-	34.2	17.9	−0.65	<0.05
70	14.1	370.8	−0.95	<0.001	174.9	101.9	−0.65	<0.05
90	3.3	5.1	−0.66	<0.01	2.6×10^5	n.s.[b]	−0.40	-

[a]The r and P values indicate the calculated regression coefficient and the significance of the relationship between CH_4 concentration and time, respectively.
[b]n.s. indicates not significant ($P > 0.05$).

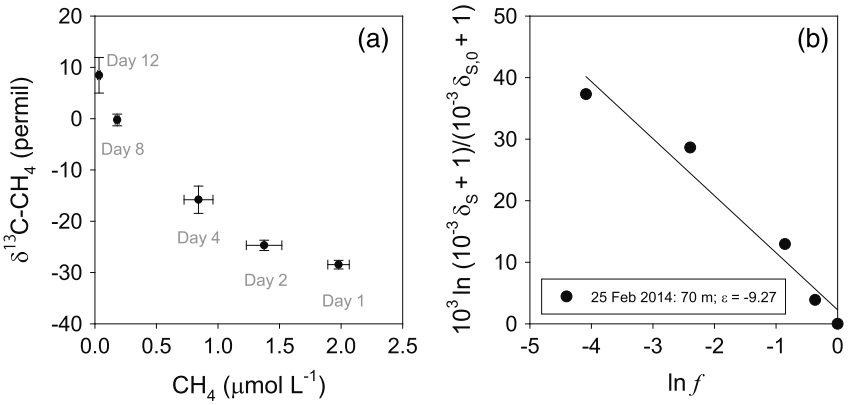

Figure 6. (a) Changes in the CH_4 concentration and δ^{13}C-CH_4 values and (b) the Rayleigh plot of CH_4 data from the incubation experiment with the addition of CH_4 gas in February 2014. Parameter *f* is the fraction of methane remaining, with respect to the initial CH_4 concentration. The slope of the linear regressions is equivalent to the isotope enrichment factor (see equation (1)).

2.4–92.6 μmol m^{-2} d^{-1} and 2.44–71.8 μmol m^{-2} d^{-1} for the 1 and 11 day running means, respectively (Figure 7c). Although the range of estimated diffusive fluxes differed between these formulas, the seasonal patterns were similar. For both estimations, the maximum diffusive CH_4 fluxes were observed in the middle of summer (August 2013), when the surface CH_4 concentration was highest.

4. Discussion

4.1. Intensity of Vertical Mixing Controlling Sedimentary CH_4 Production and Storage

Our long-term monitoring data revealed that the water surface temperature during winter significantly affected the intensity of vertical mixing and, consequently, the intensity of reducing conditions in the deeper zone of the reservoir (Figures 3a–3c). During winter 2011–2012 (December 2011–February 2012), winter mixing to below 90 m depth caused high profundal DO concentrations (Figure 2c). In contrast, weak winter mixing in winter

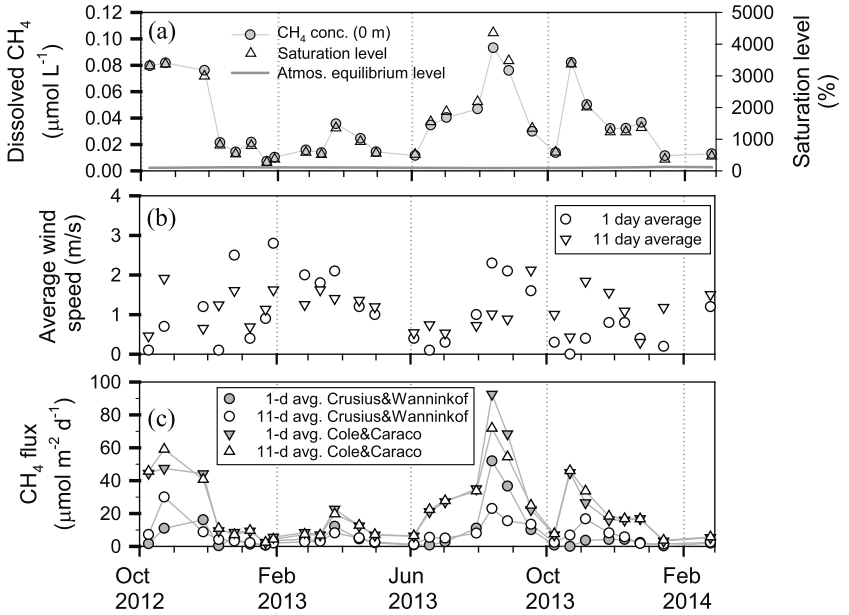

Figure 7. Seasonal variation in (a) dissolved CH_4 concentration at a depth of 0 m and its saturation level to the atmospheric equilibrium, (b) 1 and 11 day average wind speed, and (c) 1 and 11 day daily CH_4 flux using the transfer velocity (k_{600}) calculated using the formulas of *Crusius and Wanninkhof* [2003] and *Cole and Caraco* [1998].

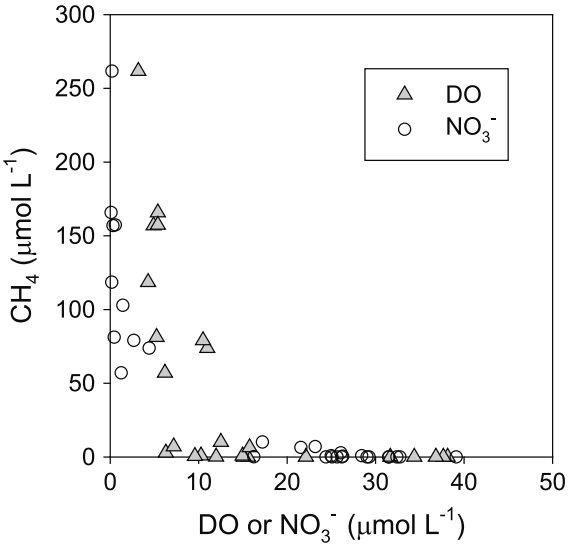

Figure 8. Biplot of DO and NO_3^- concentrations versus CH_4 concentration of water sampled at 90 m depth.

2012–2013 facilitated the development of reducing conditions in deep waters, as indicated by the depletion of profundal DO in winter and the following summer (Figures 2c and 2d).

Profundal NO_3^- concentrations decreased to zero during the strong thermal stratification period of 2013, indicating that denitrification dominated in deep waters under strong reducing conditions (Figure 2d). The depletion of profundal NO_3^- then lasted for approximately 7 months (July 2013–January 2014). Corresponding to this NO_3^- depletion, CH_4 storage developed in deep waters (Figure 4a). In general, methanogens are at a competitive disadvantage to denitrifiers as electron receptors under NO_3^--rich conditions, but they can dominate under strongly reducing conditions when NO_3^- is depleted [*Stigliani*, 1988]. In our incubation experiment, sedimentary potential CH_4 production was higher in summer 2013 than in winter 2012–2013 (Table 3), although water temperature and sediment geochemical properties did not differ between the two seasons. Potential CO_2 production during incubation exhibited similar results, suggesting that anaerobic organic matter decomposition was also higher in the sediment collected in summer. These findings support the hypothesis that the activity and/or abundance of anaerobic microorganisms (including denitrifiers) was higher in summer. This can also contribute to an increase in dissolved CO_2 concentration in the deep layer during this period. These results suggest that DO and NO_3^- depletion due to denitrification in deep waters can be an indicator of profundal CH_4 production and thus increases in CH_4 storage (Figure 8). Schematics of the effects of interannual variation in winter vertical mixing on redox condition and profundal CH_4 production in a deep subtropical reservoir are presented in Figure 9. During cold winters with higher precipitation, sufficient vertical mixing form oxic conditions at the bottom layer through increased oxygen supply from the upper layer. This is kept until next stratification period and suppresses profundal CH_4 production. In contrast, a highly reduced condition is kept at the bottom in warmer winters with insufficient vertical mixing. This facilitates methanogenic activity in the next stratification period.

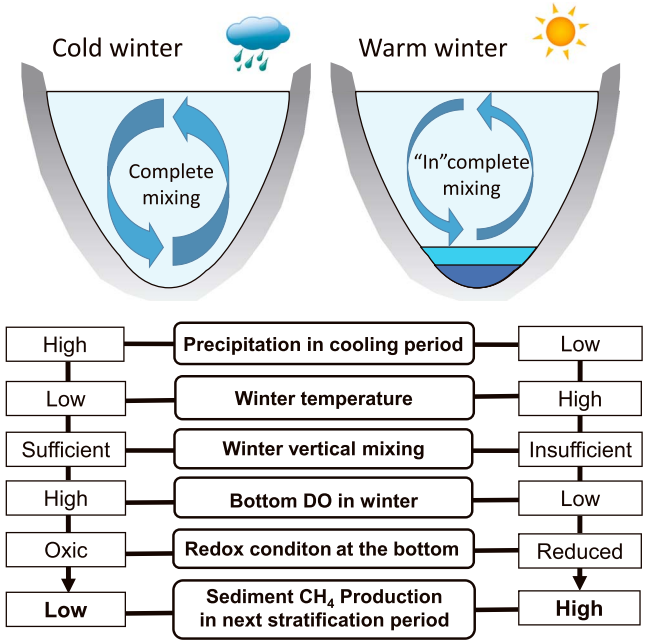

Figure 9. Schematics of the effects of interannual variation in winter vertical mixing on redox condition and profundal CH_4 production in a deep subtropical reservoir.

4.2. Water Column CH_4 Oxidation

Our profiling of δ^{13}C-CH_4 revealed that δ^{13}C values exhibited a dynamic pattern in the water column. The δ^{13}C-CH_4 values were consistently negative (-67.4 ± 0.5‰) at the near

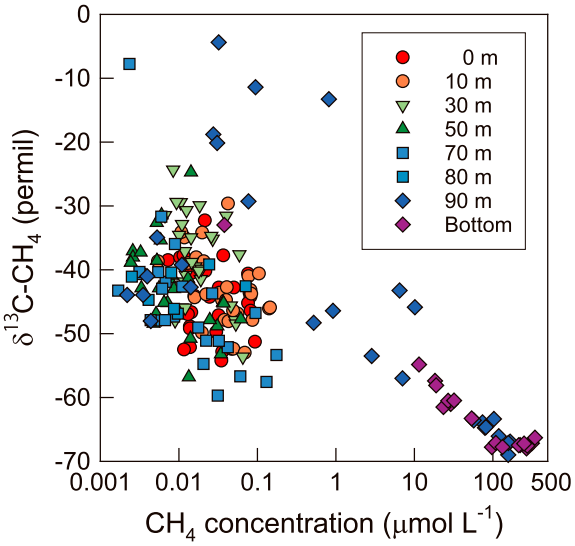

Figure 10. Biplot of CH_4 concentration versus $\delta^{13}C$ collected from all sampling depths and times.

bottom during the strong thermal stratification period when CH_4 concentrations were higher than 100 μmol L^{-1} (Figure 10). In the oxic/anoxic boundary layer that formed between depths of 70 and 90 m, the $\delta^{13}C$-CH_4 values varied substantially, suggesting that MOB preferentially oxidize $^{12}CH_4$ in this layer, resulting in a large enrichment of dissolved $^{13}CH_4$. This result was supported by our incubation experiments, which detected remarkable CH_4 oxidation activity at a depth of 70 m, at which dissolved CH_4 was enriched after the addition of CH_4 gas to the water sample (Figure 6a). Based on our experimental results, the apparent kinetic isotope enrichment factor was estimated to be −9.27 (Figure 6b), which was similar to the only available literature values from a lake in Switzerland [−8.98 to −6.89; *Blees et al*., 2014]. A slightly more positive $\delta^{13}C$-CH_4 value of near-bottom water samples during the oxic period (February–July 2013; Figure 4d) also indicates a certain degree of contribution of CH_4 oxidation at the sediment surface, given that many studies have reported the presence of anaerobic methane oxidizers in freshwater sediment (see below). Our observational and experimental results revealed the dynamic processes of CH_4 production, which could be balanced between CH_4 production in the sediment and CH_4 oxidation in both the sediment surface and the water column.

Aerobic CH_4 oxidation in the water column was unlikely to occur at a depth of 90 m, where oxygen is almost depleted, except during strong vertical mixing (Figure 2c). In this same reservoir, *Kojima et al*. [2014] recently used a catalyzed reporter deposition fluorescence in situ hybridization analysis to confirm that MOB were the predominant components of the whole bacterial community at this depth in both summer and winter. More interestingly, they identified a nitrite-dependent methane oxidizer (affiliated with the NC10 phylum) in addition to two well-characterized groups (Type I belonging to *Gammaproteobacteria* and Type II to *Alphaproteobacteria*), each of which is common in temperate and tropical lakes, respectively. These records are the first evidence of anaerobic methane oxidizers in the lake water column, although many studies have reported the presence of anaerobic methane oxidizers coupled with denitrification in freshwater sediment [*Raghoebarsing et al*., 2006; *Ettwig et al*., 2009, 2010; *Deutzmann et al*., 2014; *Norði and Thamdrup*, 2014]. In a deep meromictic tropical lake (Lake Kivu) in eastern Africa, *Borges et al*. [2011] reported nearly the same vertical trend in CH_4 concentrations as that observed during the strong stratification period in our reservoir. In their lake, maximum CH_4 concentrations (300–400 μmol L^{-1}) occurred at the deepest sampling depth (70–80 m) and decreased toward the surface. *Borges et al*. [2011] also suggested that this vertical distribution was a typical characteristic of stratified lakes due to CH_4 removal by bacterial oxidation in the water column. This finding is consistent with our observation that CH_4 accumulated during the strong stratification period but mostly disappeared within 30 m upward from the sediment. Using carbon stable isotope analysis ($\delta^{13}C$-CH_4), *Morana et al*. [2015] recently demonstrated that MOB oxidized most of the upward flux of CH_4 within the water column of an oxycline in Lake Kivu. However, in Lake Kivu, anaerobic MOB were not examined. Given previous evidence of NC10 activity in the anaerobic water column in the FTR [*Kojima et al*., 2014], further study of anaerobic methane oxidizers in tropical lakes will be needed to thoroughly understand MOB activity in lake ecosystems. Although we were unable to estimate the relative contribution of anaerobic MOB to the profundal CH_4 oxidation dynamics on the basis of $\delta^{13}C$-CH_4 values due to a lack of empirical data, the presence of anaerobic MOB may be a characteristic of tropical and subtropical lakes with anoxic deep layers. To evaluate their roles in the carbon and nitrogen cycling of subtropical and tropical lake ecosystems, further studies must examine the isotopic fractionation of $\delta^{13}C$-CH_4 and $\delta^{15}N$-NO_3^- during CH_4 oxidation and denitrification, respectively.

4.3. Source of CH_4 Emission From the Water Surface

We estimated that the diffusive CH_4 flux from the water surface increased to 92.6 μmol m^{-2} d^{-1} in midsummer (Figure 7c). Our estimations of diffusive CH_4 flux in the FTR were lower by 1 order of magnitude than the value observed from the subsurface of a shallower tropical reservoir (~35 m depth) in French Guiana [*Guérin and Abril*, 2007]. Our estimations were also lower by 1–2 orders of magnitude than those observed from the subsurface of shallower Asian subtropical reservoirs (19 m and 14 m depth) in Laos [*Chanudet et al*., 2011]. Unlike shallow lakes, CH_4 emissions due to ebullition appear to be negligible in the FTR, because the reservoir is deep enough for bubbles to dissolve in the water column [*McGinnis et al*., 2006; *Schmid et al*., 2007] and in small shallow areas with steep shores (Figure 1), where high CH_4 production and ebullition may occur. In addition to the detection of CH_4 oxidation at a depth of 30 m in winter 2012–2013 (December 2012; Table 4), the middle layer exhibited considerably lower CH_4 concentrations and much more positive δ^{13}C-CH_4 values at depths of 30 and 50 m than values in the sediment; this finding also provides evidence of CH_4 oxidation in both this and/or deeper layers (Figure 5b). Therefore, the diffusive emission from profundal CH_4 storage was unlikely to greatly contribute to atmospheric emissions, even during the strong thermal stratification period with high CH_4 concentrations in deep waters. However, we may need to pay attention to the possibility of increases in CO_2 emissions from water surface by considering high profundal CO_2 production potential during the stratification period and conversion from CH_4 to CO_2 by MOB in the water column.

We observed another peak of dissolved CH_4 in a subsurface layer (10 m depth) in midsummer that was a significantly higher concentration than concentrations at 30 and 50 m depth; however, this layer was highly oxygenated by phytoplankton photosynthesis (Figures 2c and 4b). The CH_4 concentration of this layer was much higher than both the value in the surface water and the theoretical value at atmospheric equilibrium (Figures 4b and 7a). Although we did not conduct direct measurements of flux, our estimated diffusive CH_4 flux from the water surface indicated that high CH_4 flux could occur only under conditions of high CH_4 concentration in subsurface water and high wind speed (Figure 7). Considering that the subsurface CH_4 concentration did not originate from profundal CH_4, CH_4 in the subsurface zone (and not profundal CH_4) likely serves as a major source of CH_4 emission from the water surface in the FTR.

Recently, subsurface maximum of CH_4 in the oxygenated subsurface layer has been reported for some oceans and lakes [*Reeburgh*, 2007; *Karl et al*., 2008; *Conrad*, 2009; *Grossart et al*., 2011; *Tang et al*., 2014]. Marine studies suggested that CH_4 is aerobically produced as a by-product of methylphosphonate decomposition for nitrogen fixers to obtain phosphate under nutrient-limited conditions [e.g., *Karl et al*., 2008]. In an ecosystem-scale experiment, *Bogard et al*. [2014] reported that CH_4 production in oxic surface lake water could be a major source of CH_4 emission from the lake surface. These authors also concluded that this CH_4 was produced by acetoclastic methanogenesis and was related to pelagic algal dynamics. *Bogard et al*. [2014] documented a strong link between pelagic gross primary product and net ecosystem production. As is often the case in well-stratified tropical lakes [*Verburg et al*., 2003], cyanobacterial blooms frequently occur during the summer in the FTR. Based on our isotopic data, δ^{13}C-CH_4 values at 10 m depth during summer 2013 did not significantly differ from those at 0, 30, and 50 m depths, likely due to high variability of δ^{13}C-CH_4 values (Figure 4d). These results suggest that both CH_4 production in the subsurface layer and fractionation by CH_4 oxidation affect the δ^{13}C-CH_4 values. Deep subtropical lakes have well-developed oxygenated layers and thus have a high potential for CH_4 oxidation; therefore, subsurface aerobic CH_4 production, rather than profundal anaerobic CH_4 production, may account for a large portion of CH_4 emission from the water surface.

5. Conclusions

With the progression of global warming, subtropical lakes are expected to experience not only stronger and longer thermal stratification in summer but also incomplete vertical mixing in winter, resulting in profundal hypoxia [*Sahoo and Schladow*, 2008; *Yoshimizu et al*., 2010]. Our long-term observations demonstrate that such a projection is true for the deep FTR, where the intensity of winter vertical mixing varies with climatic conditions. Based on our vertical and seasonal profiling of CH_4 concentrations and δ^{13}C values, weak winter mixing may increase sedimentary CH_4 production and thus profundal CH_4 storage through hypoxia

during the thermal stratification period. This process can enhance surface CH_4 emission, especially in shallow lakes. In an Amazonian tropical lake, *Marotta et al.* [2014] reported that anaerobic biological CH_4 production in the sediments increased exponentially in response to increased temperature. Such responses can also affect CH_4 accumulation at the lake bottom with global warming. On the other hand, our observations suggested that strong stratification (under a warmer climate) may not always increase atmospheric CH_4 emissions, because incomplete vertical mixing also promotes MOB activity in both aerobic and anaerobic layers by increasing the possibility for contact with substrates. This is especially true for lakes like the FTR that are deep enough to support MOB activity. An increase in the number of warming years may increase atmospheric CH_4 emission by building up the CH_4 accumulating layer and thinning the oxygenated layer for MOB activity. Our results suggest that the effects of interannual variation in winter mixing (and hence CH_4 production and oxidation processes) should be considered to better understand temporal variation and future trends of CH_4 dynamics in lake ecosystems.

Acknowledgments

We thank anonymous reviewers for their valuable comments on an earlier draft of this manuscript. We also thank Chih-Chung Chang (Academia Sinica, Taiwan) for providing laboratory equipment and for helpful discussions, the members of the laboratory of Fuh-Kwo Shiah, and the administration office of the Fei-Tsui Reservoir for helping with the observations and analyses. The study was conducted using the Cooperative Research Facilities (Isotope Ratio Mass Spectrometer) of the Center for Ecological Research, Kyoto University. This work was supported by the Ministry of Education, Culture, Sports, Science, and Technology for Science Research (24405007, 15H05625) in Japan, Research Institute for Humanity and Nature (RIHN project: D-06), Japan and the Kyoto University Research Development Program. The data used in this paper are available by contacting the corresponding author.

References

Abril, G., F. Guérin, S. Richard, R. Delmas, C. Galy-Lacaux, P. Gosse, A. Tremblay, L. Varfalvy, M. A. dos Santos, and B. Matvienko (2005), Carbon dioxide and methane emissions and the carbon budget of a 10 years old tropical reservoir (Petit-Saut, French Guiana), *Global Biogeochem. Cycles*, *19*, GB4007, doi:10.1029/2005GB002457.

Barros, N., J. J. Cole, L. Tranvik, Y. T. Prairie, D. Bastviken, V. L. M. Huszar, P. D. Giorgio, and F. Roland (2011), Carbon emission from hydroelectric reservoirs linked to reservoir age and latitude, *Nat. Geosci.*, *4*, 593–596, doi:10.1038/NGEO1211.

Bastviken, D., J. Ejlertsson, and L. Tranvik (2002), Measurement of methane oxidation in lakes: A comparison of methods, *Environ. Sci. Technol.*, *36*, 3354–3361.

Bastviken, D., L. J. Tranvik, J. A. Downing, P. M. Crill, and A. Enrich-Prast (2011), Freshwater methane emissions offset the continental carbon sink, *Science*, *331*, 50, doi:10.1126/science.1196808.

Blees, J., H. Niemann, C. B. Wenk, J. Zopfi, C. J. Schubert, M. K. Kirf, M. L. Veronesi, C. Hitz, and M. F. Lehmann (2014), Micro-aerobic bacterial methane oxidation in the chemocline and anoxic water column of deep south-Alpine Lake Lugano (Switzerland), *Limnol. Oceanogr.*, *59*, 311–324.

Bogard, M. J., P. A. del Giorgio, L. Boutet, M. C. G. Chaves, Y. T. Prairie, A. Merante, and A. M. Derry (2014), Oxic water column methanogenesis as a major component of aquatic CH_4 fluxes, *Nat. Commun.*, *5*, 5350, doi:10.1038/ncomms6350.

Borges, A. V., B. Delille, and L.-S. Schiettecatte (2004), Gas transfer velocities of CO_2 in three European estuaries (Randers Fjord, Scheldt, and Thames), *Limnol. Oceanogr.*, *49*, 1630–1641.

Borges, A. V., G. Abril, B. Delille, J.-P. Descy, and F. Darchambeau (2011), Diffusive methane emissions to the atmosphere from Lake Kivu (Eastern Africa), *J. Geophys. Res.*, *116*, G03032, doi:10.1029/2011JG001673.

Chanudet, V., S. Descloux, and A. Harby (2011), Gross CO_2 and CH_4 emissions from the Nam Ngum and Nam Leuk subtropical reservoirs in Lao PDR, *Sci. Total Environ.*, *409*, 5382–5391.

Chen, H., X. Yuan, Z. Chen, Y. Wu, X. Liu, D. Zhu, N. Wu, Q. Zhu, C. Peng, and W. Li (2011), Methane emissions from the surface of the Three Gorges Reservoir, *J. Geophys. Res.*, *116*, D21306, doi:10.1029/2011JD016244.

Chen, Y. J. C., S. C. Wu, B. S. Lee, and C. C. Hung (2006), Behavior of storm-induced suspension interflow in subtropical Feitsui Reservoir, Taiwan, *Limnol. Oceanogr.*, *51*, 1125–1133.

Chou, W.-S., T.-C. Lee, J.-Y. Lin, and S.-L. Yu (2007), Phosphorus load reduction goals for Feitsui Reservoir watershed, Taiwan, *Environ. Monit. Assess.*, *131*, 395–408.

Ciais, P., et al. (2013), Carbon and Other Biogeochemical Cycles, in *Climate Change 2013: The Physical Science Basis. Contribution of Working Group I to the Fifth Assessment. Report of the Intergovernmental Panel on Climate Change*, edited by T. F. Stocker et al., pp. 465–570, Cambridge Univ. Press, Cambridge.

Cole, J. J., and N. F. Caraco (1998), Atmospheric exchange of carbon dioxide in a low-wind oligotrophic lake measured by the addition of SF6, *Limnol. Oceanogr.*, *43*, 647–656, doi:10.4319/lo.1998.43.4.0647.

Conrad, R. (2009), The global methane cycle: Recent advances in understanding the microbial processes involved, *Environ. Microbiol. Rep.*, *1*, 285–292.

Crusius, J., and R. Wanninkhof (2003), Gas transfer velocities measured at low wind speed over a lake, *Limnol. Oceanogr.*, *48*, 1010–1017.

Deutzmann, J. S., P. Stief, J. Brandes, and B. Schink (2014), Anaerobic methane oxidation coupled to denitrification is the dominant methane sink in a deep lake, *Proc. Natl. Acad. Sci. U.S.A.*, *111*, 18,273–18,278, doi:10.1073/pnas.1411617111.

Ettwig, K. F., T. Van Alen, K. T. van de Pas-Schoonen, M. S. M. Jetten, and M. Strous (2009), Enrichment and molecular detection of denitrifying methanotrophic bacteria of the NC10 phylum, *Appl. Environ. Microbiol.*, *75*, 3656–3662, doi:10.1128/AEM.00067-09.

Ettwig, K. F., et al. (2010), Nitrite-driven anaerobic methane oxidation by oxygenic bacteria, *Nature*, *464*(7288), 543–548, doi:10.1038/nature08883.

Grossart, H.-P., K. Frindte, C. Dziallas, W. Eckert, and K. W. Tang (2011), Microbial methane production in oxygenated water column of an oligotrophic lake, *Proc. Natl. Acad. Sci. U.S.A.*, *108*, 19,657–19,661.

Guérin, F., and G. Abril (2007), Significance of pelagic aerobic methane oxidation in the methane and carbon budget of a tropical reservoir, *J. Geophys. Res.*, *112*, G03006, doi:10.1029/2006JG000393.

Guérin, F., G. Abril, D. Serça, C. Delon, S. Richard, R. Delmas, A. Tremblay, and L. Varfalvy (2007), Gas transfer velocities of CO_2 and CH_4 in a tropical reservoir and its river downstream, *J. Mar. Syst.*, *66*, 161–172.

IPCC (2013), *Climate Change 2013: The Physical Science Basis. Working Group I Contribution to the Fifth Assessment Report of the Intergovernmental Panel on Climate Change*, pp. 1535, Cambridge Univ. Press, Cambridge, U. K., and New York.

Itoh, M., N. Ohte, K. Koba, A. Sugimoto, and M. Tani (2008), Analysis of methane production pathways in a riparian wetland of a temperate forest catchment, using $\delta^{13}C$ of pore water CH_4 and CO_2, *J. Geophys. Res.*, *113*, G03005, doi:10.1029/2007JG000647.

Itoh, M., et al. (2011), Mitigation of methane emissions from paddy fields by prolonging midseason drainage, *Agric., Ecosyst. Environ.*, *141*, 359–372, doi:10.1016/j.agee.2011.03.019.

Jähne, B., G. Heinz, and W. Dietrich (1987), Measurement of the diffusion coefficients of sparingly soluble gases in water, *J. Geophys. Res.*, *92*, 10,767–10,776, doi:10.1029/JC092iC10p10767.
Karl, D. M., L. Beversdorf, K. M. Björkman, M. J. Church, A. Martinez, and E. F. Delong (2008), Aerobic production of methane in the sea, *Nat. Geosci.*, *1*, 473–478, doi:10.1038/ngeo234.
Kojima, H., R. Tokizawa, K. Kogure, Y. Kobayashi, M. Itoh, F.-K. Shiah, N. Okuda, and M. Fukui (2014), Community structure of planktonic methane-oxidizing bacteria in a subtropical reservoir characterized by dominance of phylotype closely related to nitrite reducer, *Sci. Rep.*, *4*, 5728.
Liss, P. S., and L. Merlivat (1986), Air-sea exchange rates: Introduction and synthesis, in *The Role of Air-Sea Exchange in Geochemical Cycling*, edited by P. Buat-Ménard, pp. 113–127, Reidel, Dordrecht.
Mariotti, A., J. C. Germon, P. Hubert, P. Kaiser, R. Letolle, A. Tardieux, and P. Tardieux (1981), Experimental determination of nitrogen kinetic isotope fractionation: Some principles; illustrations for the denitrification and nitrification processes, *Plant Soil*, *62*, 413–430, doi:10.1007/BF02374138.
Marotta, H., L. Pinho, C. Gudasz, D. Bastviken, L. J. Tranvik, and A. Enrich-Prast (2014), Greenhouse gas production in low-latitude lake sediments responds strongly to warming, *Nat. Clim. Change*, *4*, 2222.
McAuliffe, C. (1971), GC determination of solutes by multiple phase equilibration, *Chemtech*, *1*, 46–51.
Mcginnis, D. F., J. Greinert, Y. Artemov, S. E. Beaubien, and A. Wëst (2006), Fate of rising methane bubbles in stratified waters: How much methane reaches the atmosphere?, *J. Geophys. Res.*, *111*, C09007, doi:10.1029/2005JC003183.
Morana, C., A. V. Borges, F. A. E. Roland, F. Darchambeau, J.-P. Descy, and S. Bouillon (2015), Methanotrophy within the water column of a large meromictic tropical lake (Lake Kivu, East Africa), *Biogeosciences*, *12*, 2077–2088.
Norði, K., and B. Thamdrup (2014), Nitrate-dependent anaerobic methane oxidation in a freshwater sediment, *Geochim. Cosmochim. Acta*, *132*, 141–150.
Parsons, T. R., Y. Maita, and C. M. Lalli (1984), *A Manual of Chemical and Biological Methods for Seawater Analysis*, pp. 173, Pergamon Press, New York.
Pasche, N., M. Schmid, F. Vazquez, C. Schubert, A. Wüest, J. D. Kessler, M. A. Pack, W. S. Reeburgh, and H. Bürgmann (2011), Methane sources and sinks in Lake Kivu, *J. Geophys. Res.*, *116*, G03006, doi:10.1029/2011JG001690.
Raghoebarsing, A. A., et al. (2006), A microbial consortium couples anaerobic methane oxidation to denitrification, *Nature*, *440*, 918–921.
R Development Core Team (2012), R: A Language and Environment for Statistical Computing, R Foundation for Statistical Computing, Vienna, Austria. [Available at http://www.R-project.org/.]
Reeburgh, W. S. (2007), Oceanic methane biogeochemistry, *Chem. Rev.*, *107*, 486–513, doi:10.1021/cr050362v.
Sahoo, G. B., and S. G. Schladow (2008), Impacts of climate change on lakes and reservoirs dynamics and restoration policies, *Sustain. Sci.*, *3*, 189–199.
Schmid, M., et al. (2007), Sources and sinks of methane in Lake Baikal: A synthesis of measurements and modeling, *Limnol. Oceanogr.*, *52*, 1824–1837.
Schubert, C. J., T. Diem, and W. Eugster (2012), Methane emissions from a small wind shielded lake determined by eddy covariance, flux chambers, anchored funnels, and boundary model calculations: A comparison, *Environ. Sci. Technol.*, *46*, 4515–4522.
Stigliani, W. M. (1988), Changes in values "Capacities" of soils and sediments as indicators of nonlinear and time-delayed environmental effects, *Environ. Monit. Assess.*, *10*, 245–307.
Sugimoto, A. (1996), GC/GC/C/IRMS system for carbon isotope measurement of low level methane concentration, *Geochem. J.*, *30*, 195–200.
Tang, K. W., D. F. McGinnis, K. Frindte, V. Brüchert, and H.-P. Grossart (2014), Paradox reconsidered: Methane oversaturation in well-oxygenated lake waters, *Limnol. Oceanogr.*, *59*, 275–284.
Teodoru, C. R., et al. (2012), The net carbon footprint of a newly created boreal hydroelectric reservoir, *Global Biogeochem. Cycles*, *26*, GB2016, doi:10.1029/2011GB004187.
Tokida, T., Y. Nakajima, K. Hayashi, Y. Usui, N. Katayanagi, M. Kajiura, H. Nakamura, and T. Hasegawa (2014), Fully automated, high-throughput instrumentation for measuring the $\delta^{13}C$ of methane and application of the instrumentation to rice paddy samples, *Rapid Commun. Mass Spectrom.*, *28*, 2315–2324, doi:10.1002/rcm.7016.
Vachon, D., and P. A. del Giorgio (2014), Whole-lake CO_2 dynamics in response to storm events in two morphologically different lakes, *Ecosystems*, *17*, 1338–1353, doi:10.1007/s10021-014-9799-8.
Verburg, P., R. E. Hecky, and H. Kling (2003), Ecological consequences of a century of warming in Lake Tanganyika, *Science*, *301*, 505–507.
Wanninkhof, R. (1992), Relationship between gas exchange and wind speed over the ocean, *J. Geophys. Res.*, *97*, 7373–7382, doi:10.1029/92JC00188.
Wiesenburg, D. A., and N. L. Guinasso (1979), Equilibrium solubilities of methane, carbon-monoxide, and hydrogen in water and seawater, *J. Chem. Eng. Data*, *24*, 356–360, doi:10.1021/je60083a006.
Xiao, S., D. Liu, Y. Wang, Z. Yang, and W. Chen (2013), Temporal variation of methane flux from Xiangxi Bay of the Three Gorges Reservoir, *Sci. Rep.*, *3*, 2500.
Yoshimizu, C., K. Yoshiyama, I. Tayasu, T. Koitabashi, and T. Nagata (2010), Vulnerability of a large monomictic lake (Lake Biwa) to warm winter event, *Limnology*, *11*, 233–239.